J Therm Anal Calorim (2011) 104:1045–1050
DOI 10.1007/s10973-010-1164-3

Kinetic analysis of the thermal decomposition of copper (I) complexes with heterocyclic thiones

K. Chrissafis · M. Lalia-Kantouri · P. Aslanidis

Received: 29 September 2010 / Accepted: 3 November 2010 / Published online: 8 December 2010

Abstract Two series of copper (I) halide complexes formulated as $[(L)CuX(\mu_2\text{-}L)_2CuX(L)]$ and $[(L)_2Cu(\mu_2\text{-}L)_2Cu(L)_2]^{2+}\ 2X^-$, respectively (X = Cl, Br and L = 4,6-dimethylpyrimidine-2-thione (dmpymtH)) were prepared. From the thermogravimetric curves it was found that among the four studied materials, $[Cu_2(dmpymtH)_6]^{2+}2Cl^-$ presents a lower thermal stability. For the determination of the activation energy (E) two different methods have been used comparatively, since every method has its own error. These methods were the isoconversional methods of Ozawa, Flynn and Wall (OFW), and Friedman. The dependence of the E on the value of the mass conversion α, as calculated with OFW and Friedman's methods, can be separated in three distinct regions. The decomposition mechanism is very complex and can be described using at least three different mechanisms with different activation energies. The best fitting of experimental data with theoretical models gave nth-order for all the three mechanisms (Fn–Fn–Fn).

Keywords Copper(I) complexes · Heterocyclic thiones · TG/DTG–DTA · Activation energy · Kinetics

K. Chrissafis (✉)
Solid State Physics Department,
School of Physics, Aristotle University of Thessaloniki,
54124 Thessaloniki, Greece
e-mail: hrisafis@physics.auth.gr

M. Lalia-Kantouri · P. Aslanidis
Laboratory of Inorganic Chemistry,
Department of Chemistry, Faculty of Sciences, Aristotle
University of Thessaloniki, Thessaloniki 54124, Greece

Introduction

The interaction of heterocyclic thiones with many transition metals has been an intense area of study for the last few decades, as certain of these thioamides have shown interesting biochemical properties or are found to be present in the active sites of many metalloproteins [1, 2]. Extensive investigations in this area have been concerned with complexes of the monovalent coinage metals Cu and Ag, whereby the high flexibility of the closed-shell d^{10} metal ions and the versatility of the thione ligands resulted in an extraordinary variety of molecular structures [3–5]. In fact, the structural features and composition of such complexes mainly depend on factors like steric demands on the part of the ligands and, in the particular case of metal halide complexes, on electronic effects introduced by the halide donor, but also on the reaction conditions applied, e.g., metal/thione ratio, reaction temperature, and solvent. In this context, apart from the common three or four-coordinate complexes, neutral doubly bridged dinuclear species of the general formula $[CuX(thione)_2]_2$ [6] or cationic with the general formula $[Cu_2(thione)_6]^{2+}\ 2X^-$ (X = Cl, Br) [7] were observed.

Much attention has also been paid to emissive copper (I) complexes in view of practical applications in solar-energy conversion systems, chemical sensors, or display devises [8–10]. However, most of the studies about copper (I) complexes with thiones as ligands are limited to the structural aspects, and reports on their thermal stability and the kinetic description are rare [6, 7].

Since it is very interesting to reveal the impact of the thione ligands on the thermal stability and the decomposition kinetics of such complexes, two series of copper (I) halide complexes formulated as $[(L)CuX(\mu_2\text{-}L)_2CuX(L)]$ and $[(L)_2Cu(\mu_2\text{-}L)_2Cu(L)_2]^{2+}\ 2X^-$, respectively (X = Cl,

Br and L = 4,6-dimethylpyrimidine-2-thione (dmpymtH)) were studied and presented in this work.

Experimental

Commercially available copper(I) and copper(II) halides were purchased as reagent grade from Aldrich and were used without further purification, while the thione ligands were re-crystallized from hot ethanol prior to their use. All the solvents were purified by respective suitable methods and allowed to stand over molecular sieves.

General procedure for the synthesis of the neutral Cu(I) complexes $[CuXL_2]_2$

The complexes were prepared according to published procedures [6, 7], in some cases slightly modified. A suspension of 0.5 mmol of copper(I) halide (49.5 mg for CuCl, 71.7 mg for CuBr) in 50 cm^3 of dry acetonitrile was stirred for 2 h at 50 °C. The resulting clear solution was treated with a solution of the appropriate thione (0.5 mmol) dissolved in a small amount (~20 mL) of ethanol or methanol and the new reaction mixture was stirred for additional 30 min at 50 °C. Slow evaporation of the clear solution at ambient temperature resulted in a microcrystalline solid, which was filtered off and dried in vacuum. The compounds are moderately soluble in CH_3CN, CH_3COCH_3, and $CHCl_3$.

N1: $[CuCl(dmpymtH)_2]_2$

Orange microcrystalline solid, yield 55.0%. Stoichiometry calculated for $C_{24}H_{32}Cl_2Cu_2N_8S_4$: C, 37.99; H, 4.25; Cu, 16.75; N, 14.77. Found: C, 38.25; H, 4.35; Cu, 16.27; N, 14.82%.

N2: $[CuBr(dmpymtH)_2]_2$

Orange microcrystalline solid, yield 46.4%. Stoichiometry calculated for $C_{24}H_{32}Br_2Cu_2N_8S_4$: C, 34.0; H, 3.80; Cu, 14.99; N, 13.22. Found: C, 35.25; H, 3.93; Cu, 14.79; N, 12.85%.

General procedure for the synthesis of the Cu(I) cationic complexes $[Cu_2L_6]^{2+}$ $2X^-$

The complexes were prepared according to the following procedures [6, 7]. A solution of 0.5 mmol of copper (II) chloride or bromide in 10 mL of water was treated with an ethanolic solution of the appropriate thione (2.5 mmol in 20 mL) and the resulting mixture was stirred for 30 min at ambient temperature. The resulting clear solution was kept at 5 °C until a microcrystalline solid was formed, which was filtered off and dried in vacuum. The compounds are soluble in CH_3NO_2, CH_3OH, CH_3COCH_3, and CH_2Cl_2.

N3: $[Cu_2(dmpymtH)_6]^{2+}$ $2Cl^-$

Orange to red microcrystalline solid, yield 68.0%. Stoichiometry calculated for $C_{36}H_{48}Cl_2Cu_2N_{12}S_6$: C, 41.60; H, 4.62; Cu, 12.23; N, 16.17. Found: C, 40.99; H, 4.74; Cu, 12.43; N, 15.85%. Conductivity in CH_3NO_2 (Λ = 151.3 μS cm^{-1}).

N4: $[Cu_2(dmpymtH)_6]^{2+}$ $2Br^-$

Orange to red microcrystalline solid, yield 60.6%. Stoichiometry calculated for $C_{36}H_{48}Br_2Cu_2N_{12}S_6$: C, 38.33; H, 4.38; Cu, 11.27; N, 14.90. Found: C, 38.08; H, 3.99; Cu, 11.38; N, 14.67%. Conductivity in CH_3NO_2 (Λ = 148.7 μS cm^{-1}).

Thermogravimetric analysis was carried out with a SETARAM SETSYS TG-DTA 16/18. Samples (6.0 ± 0.2 mg) were placed in alumina crucibles. An empty alumina crucible was used as reference. The compounds were heated from ambient temperature to 450 °C in a 50 mL min^{-1} flow of N_2 at heating rates 5, 10, 20 °C min^{-1}. Continuous recordings of sample temperature, sample weight, its first derivative and heat flow were taken.

Results and discussion

The TG and derivative thermogravimetric (DTG) curves of the sample N1 for heating rate β = 10 °C min^{-1} are shown in Fig. 1. At about 161 °C, the studied sample began to decompose and completed the decomposition at about 425 °C; its maximum decomposition rate was at 250 °C

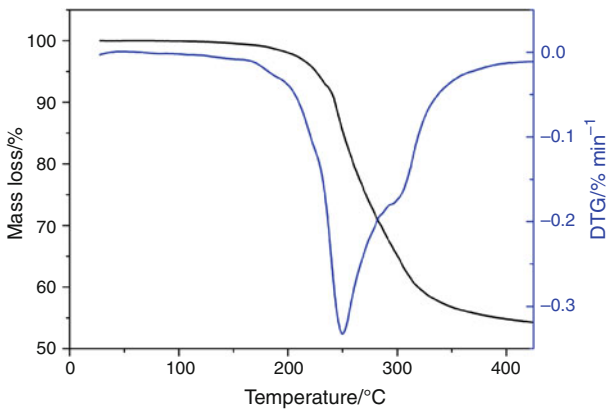

Fig. 1 Mass loss and derivative mass loss curves of sample N1 for heating rate β = 10 °C min^{-1}

while the second overlapped peak has a maximum at 298 °C. The other three studied samples also have a complicated mass loss with overlapped peaks at the DTG curve. The temperatures at which the studied materials begin to decompose are: 170, 133, and 180 °C for the samples N2, N3, and N4, respectively. So, from the thermogravimetric curves it was found that among the four studied materials, sample N3 presents a lower thermal stability than the rest three. The maximum decomposition rate was at about 249 ± 1 °C for the other three samples.

In order to determine the kinetic mechanisms of the decomposition of the studied materials different heating rates are used. The mass loss for heating rates 5, 10, and 20 °C min^{-1} is shown in Fig. 2 for the sample N4. The TG curves shifted to higher temperatures as the heating rate (β) increased from 5 to 20 °C min^{-1}. The onset shifts to higher temperatures with increasing β due to the shorter time required for the sample to reach a given temperature at faster heating rates. This β dependence was also indicated by the DTG curves (Fig. 3), with the DTG peaks shifting towards higher temperatures with increasing β. The other studied samples present analogous dependence from the heating rate.

For the determination of the activation energy using multiple heating rates the isoconversional methods are used. Since every isoconversional method has different errors, the use of more than one method can give a range of values for the activation energy at every particular value of α.

The Ozawa–Flynn–Wall (OFW) [11, 12] method involves the measurement of the temperature T, corresponding to a fixed value of the degree of conversion α (partial mass loss), from the experiments at different heating rates β. The OFW method is based on the following equation:

$$\ln \beta = -1.0516 \frac{E}{RT} + \text{const}$$

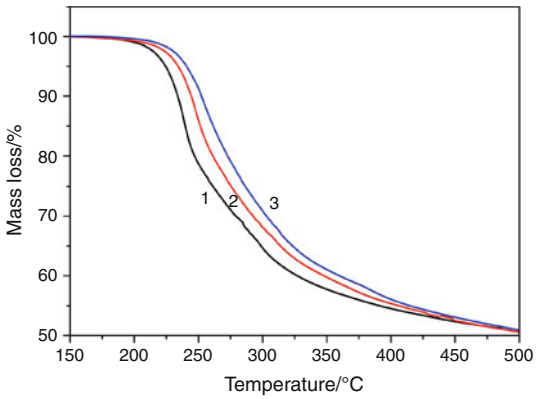

Fig. 2 Mass loss curves of sample N4 for heating rates. *1* $\beta = 5$, *2* $\beta = 10$, *3* $\beta = 20$ °C min^{-1}

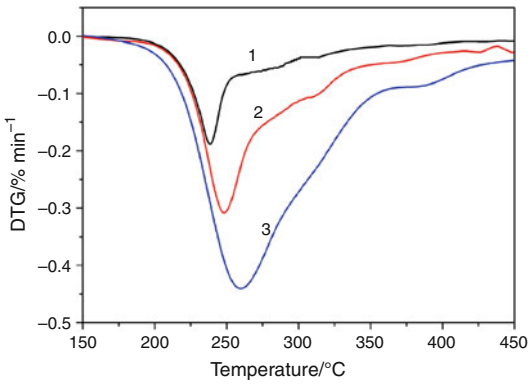

Fig. 3 Derivative mass loss curves of sample N4 for heating rates. *1* $\beta = 5$, *2* $\beta = 10$, *3* $\beta = 20$ °C min^{-1}

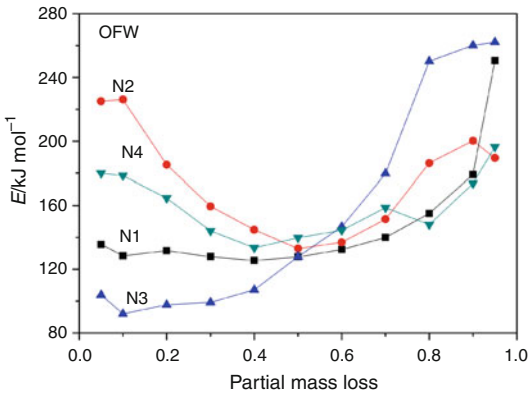

Fig. 4 Activation energy E, as calculated with OFW method, versus degree of conversion α

where E the activation energy, β the heating rate, and R the gas constant. The plot of $\ln\beta$ vs. $1/T$ gives the slope $-1.0516\ E/R$ by which the activation energy has been evaluated. If the determined activation energy is the same for the various values of α, the existence of a single-step reaction can be concluded with certainty. On the contrary, a change of E with increasing degree of conversion is an indication of a complex reaction mechanism that invalidates the separation of variables involved in the OFW analysis [13]. These complications are significant, especially in the case that the total reaction involves competitive mechanisms.

In Fig. 4, the dependence of the activation energy on the different conversion values as calculated by the OFW method is presented. The shape of this dependence is different from sample to sample. For the sample N1 it is obvious that E can be considered as having almost a constant average value till the value of partial mass loss 0.7 and after this the activation energy present a monotonous increase. The sample N3 has an analogous shape with the N1 sample, a shorter stable area till 0.4 and afterwards a

big increase. The shape of the dependence of E for the samples N2 and N4 is about the same. It presents first a monotonous decrease, secondly a short area of a stable value for E and afterwards an increase.

The second method that has been used is the differential isoconversional method suggested by Friedman [14] and it is based on the following equation:

$$\ln\left(\beta\frac{\mathrm{d}\alpha}{\mathrm{d}T}\right) = \ln A + \ln f(\alpha) - \frac{E}{RT}$$

where A is the pre-exponential factor, $f(\alpha)$ the conversion function (reaction model) and the meaning of the other symbols is the same as described previously. For a constant α, the plot of $\ln\left(\beta\frac{\mathrm{d}\alpha}{\mathrm{d}T}\right)$ vs. $\frac{1}{T}$ obtained from curves recorded at several heating rates, should be a straight line whose slope gives us the value of E. It is obvious from the above equation that if the function $f(\alpha)$ is constant for a particular value of α, then the sum $\ln f(\alpha) + \ln A/\beta$ is also constant.

In Fig. 5, the dependence of the activation energy on the different conversion values as calculated by the Friedman's method is presented. The differences in the values of E calculated by the OFW and Friedman methods can be explained by a systematic error due to improper integration. The method of Friedman employs instantaneous rate values being measured; therefore, it appears to be very sensitive to experimental noise. With OFW method, the equation used is derived assuming constant activation energy and by introducing systematic error in the estimation of E in the case that E varies with α, an error that can be estimated by comparison with the Friedman results [15]. The calculation of the activation energy using more than one isoconversional methods can give an area of values for every particular value of α, where the true values of E can be found.

Comparing the results of the two isoconversional methods we can conclude that due to the complicated shape of the curves to describe the decomposition of these materials at least two different decomposition mechanisms must be used.

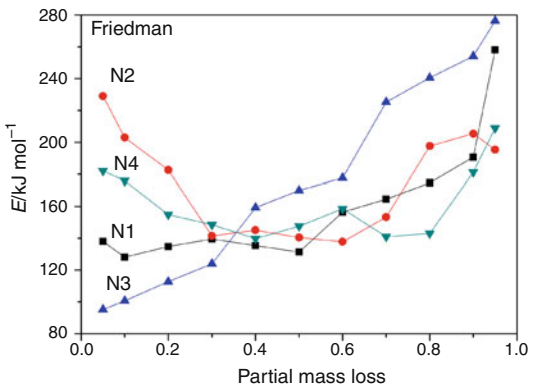

Fig. 5 Activation energy E, as calculated with Friedman's method, versus degree of conversion α

The multivariate nonlinear regression method is used for the determination of the kinetic triplet. This method applies a 6th-degree Runge–Kutta process in a modified MARQUARDT [16] procedure to solve a system of differential equations, which is essentially based on the differential equations relevant to the different reaction types and their combinations. Fundamentally, multi-step processes can only be analyzed with nonlinear regression. But nonlinear regression proves to be advantageous for one-step processes as well, because it provides a considerably better quality of fit as compared to multiple nonlinear regressions.

For this calculation 16 different kinetic models are used. The quality of the mathematical fitting depends on the regression coefficient R (Table 1). The value of E can be determined from the model corresponding to maximum R. In some cases, the so-obtained value of E is significantly different from those obtained by the isoconversional methods. Thus, using this statistical criterion it is difficult to say which model is the real one. For such cases an R-value lower than $R_{\max}$ could correspond to the true kinetic model [17]. In our case, the best kinetic model is the Fn.

In Fig. 6 is presented the plots of the fitting with the best model Fn for one of the studied materials, sample N4, as an example.

The quality of the fitting with the Fn model cannot be characterized as acceptable. The divergences which appear at the end of the mass loss in the studied area are quite obvious while small divergences are appear in the middle area of mass loss depending on the heating rate. The quality of the fitting is analogous to the other studied materials. The calculated values of E and A for the best kinetic model after the fitting for the four studied samples are presented in Table 1.

Since the quality of this fitting is not at an acceptable level, the fitting cannot be stopped here. In order to further enhance the quality of the fitting, we must consider more than one reaction mechanisms. As it has been mentioned earlier the DTG peak is multi step. This is another indication for the complex mechanism of the decomposition of these materials.

Table 1 Values of the pre-exponential factor, activation energy and reaction order

Reaction mechanism (Fn)	N1	N2	N3	N4
lg$A$	10.5	13.1	8.1	13.7
E	127.4	152.4	99.1	158.2
n	2.9	3.8	2.9	4.9
R	0.9995	0.9991	0.9970	0.9989

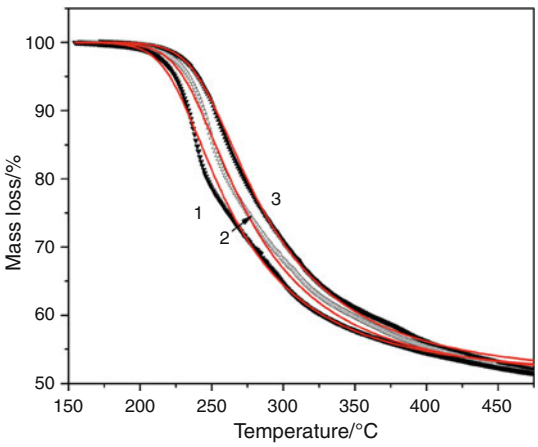

Fig. 6 Mass loss curves and fitting curves with Bna mechanism of sample N4 for heating rates. *1* $\beta = 5$, *2* $\beta = 10$, *3* $\beta = 20$ °C min^{-1}

Table 2 Values of the pre-exponential factor, activation energy and reaction order

	N1	N2	N3	N4
First mechanism (Fn)				
lg*A*	14.9	13.0	7.3	13.5
E	148.3	150.5	85.0	154.5
n	1.3	1.7	1.0	1.1
Second mechanism (Fn)				
lg*A*	11.3	16.3	16.8	10.9
E	135.4	201.8	187.4	142.9
n	2.9	4.0	4.1	4.1
R	0.9997	0.9996	0.9995	0.9994

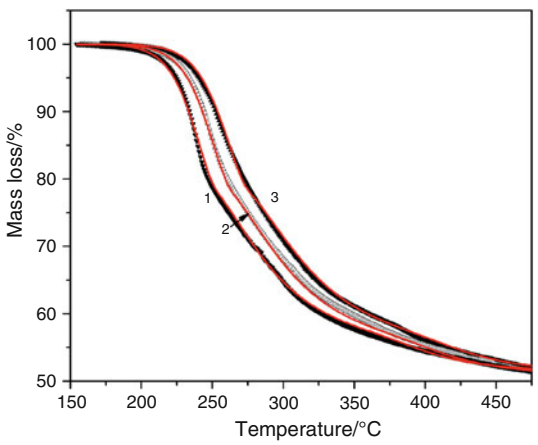

Fig. 7 Mass loss curves and fitting curves with Fn–Fn–Fn mechanisms of sample N4 for heating rates. *1* $\beta = 5$, *2* $\beta = 10$, *3* $\beta = 20$ °C min^{-1}

These reactions can be consecutive, competitive, and parallel. As it is easy to understand, the calculation of the kinetic triplet using different combinations of the reactions

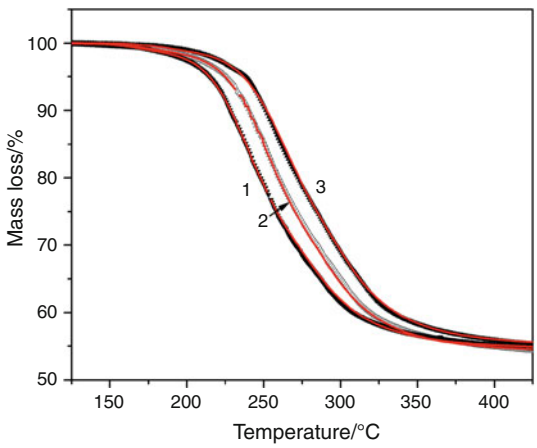

Fig. 8 Mass loss curves and fitting curves with Fn–Fn–Fn mechanisms of sample N1 for heating rates. *1* $\beta = 5$, *2* $\beta = 10$, *3* $\beta = 20$ °C min^{-1}

Table 3 Values of the pre-exponential factor, activation energy and reaction order

	N1	N2	N3	N4
First mechanism (Fn)				
lg*A*	13.6	22.8	7.4	13.5
E	133.7	221.0	85.7	153.6
n	2.2	2.7	1.2	0.7
Second mechanism (Fn)				
lg*A*	11.3	13.1	13.1	11.1
E	134.1	150.9	150.1	141.2
n	2.2	1.6	1.1	3.4
Third mechanism (Fn)				
lg*A*	20.9	15.9	23.3	13.7
E	245.9	197.6	270.0	204.3
n	4.8	3.9	4.6	2.5
R	0.9997	0.9997	0.9998	0.9997

is much more complicated now. From these combinations, we can ignore the competitive reactions, since the total mass loss for all the heating rates is the same (Fig. 2). First, two consecutive mechanisms were used for the fitting. For the determination of the kinetic model of the second mechanism only the three best models were examined: The model Fn, which is the best kinetic model at the fitting using multiple heating rates data, and the models Cn and Bna, which are autocatalysis models.

The calculated parameters (E, A, and n) of the examined mechanisms are presented in Table 2. The best fitting results for the second mechanism were obtained with Fn kinetic model. The fitting to the experimental data is better than the fitting using only one reaction mechanism. The divergences are only at the end of the mass loss area for all the studied materials.

The combination of two parallel reaction mechanisms did not improve the quality of the fitting. Since the divergences still remain at the end of the mass loss and the dependence of E on α shows that in the end there is a large increase of the activation energy, thee consecutive reaction mechanisms are used. At this step of fitting only the simplest Fn model is used. The results of the fitting now, using thee Fn models, are very good for all the studied samples. The quality of the fitting can be seen in Figs. 7 and 8 for the two of the studied materials and the calculated values are presented in Table 3.

Conclusions

From the thermogravimetric curves it was found that among the four studied materials, sample N3 presents a lower thermal stability. For the determination of the activation energy (E) two different methods have been used comparatively, since every method has its own error. These methods were the isoconversional methods of Ozawa, Flynn, and Wall (OFW) and Friedman. The dependence of the E on the value of the mass conversion α, as calculated with OFW and Friedman's methods, can be separated in three distinct regions. The decomposition mechanism is very complex and can be described using at least three different mechanisms with different activation energies. The best fitting of experimental data with theoretical models give nth order for all the three mechanisms (Fn–Fn–Fn).

References

1. Krebs B, Henkel G. Transition-metal thiolates: from molecular fragments of sulfidic solids to models for active centers in biomolecules. Angew Chem Int Ed. 1991;30:769–88.
2. Holm RH, Solomon EJ. Structural and functional aspects of metal sites in biology. Chem Rev. 1996;96:2239–314.
3. Raper ES. Complexes of heterocyclic thione donors. Coord Chem Rev. 1985;61:115–84.
4. Raper ES. Complexes of heterocyclic thioamides and related ligands. Coord Chem Rev. 1994;129:91–156.
5. Raper ES. Complexes of heterocyclic thionates. Part 1. Complexes of monodentate and chelating ligands. Coord Chem Rev. 1996;153:199–255.
6. Aslanidis P, Gaki V, Chrissafis K, Lalia-Kantouri M. Luminescence and thermal behaviour by simultaneous TG/DTG-DTA coupled with MS of neutral copper (I) complexes with heterocyclic thiones. J Therm Anal Calorim. doi:10.1007/s10973-010-974-7.
7. Aslanidis P, Chrissafis K, Lalia-Kantouri M. Luminescence and thermal behaviour of copper (I) complexes with heterocyclic thiones Part II: Cationic complexes. J Therm Anal Calorim. doi:10.1007/s10973-010-1077-1.
8. Scaltrino DV, Thompson DW, O'Callaghan JA, Meyer GJ. MLCT excited states of cuprous bis-phenanthroline coordination compounds. Coord Chem Rev. 2000;208:243–66.
9. Mc Millin DR, McNett KM. Photoprocesses of copper complexes that bind to DNA. Chem Rev. 1998;98:1201–20.
10. Armaroli N. Photoactive mono- and polynuclear Cu(I)-phenanthrolines. A viable alternative to Ru(II)-polypyridines. Chem Soc Rev. 2001;30:113–24.
11. Ozawa T. A new method of analyzing thermogravimetric data. Bull Chem Soc Jpn. 1965;38:1881–6.
12. Flynn JH, Wall LA. A quick direct method for the determination of activation energy from thermogravimetric data. Polym Lett. 1966;4:323–8.
13. Ozawa T. Kinetic analysis of derivative curves in thermal analysis. J Therm Anal. 1970;2:301–24.
14. Friedman HL. Kinetics of thermal degradation of char-forming plastics from thermogravimetry. Application to a phenolic plastic. J Polym Sci C. 1964;6:183–95.
15. Vyazovkin S. Modification of the integral isoconversional method to account for variation in the activation energy. J Comput Chem. 2001;22:178–83.
16. Opfermann J. Kinetic analysis using multivariate non-linear regression I. Basic concepts. J Therm Anal Calorim. 2000;60:641.
17. Budrugeac P, Petre AL, Segal E. Some problems concerning the evaluation of non-isothermal kinetic parameters. J Therm Anal Calorim. 1996;47:123–34.